Capacitance-voltage modeling of metal-ferroelectric-semiconductor capacitors based on epitaxial oxide heterostructures

Woong Choi, Sunkook Kim, Yong Wan Jin, Sang Yoon Lee, and Timothy D. Sands

---

Articles you may be interested in

Integration of (PbZr 0.52 Ti 0.48 O 3) on single crystal diamond as metal-ferroelectric-insulator-semiconductor capacitor
Appl. Phys. Lett. **94**, 242901 (2009); 10.1063/1.3156030

Evaluation of capacitance-voltage characteristic and memory window of metal-ferroelectric-insulator-silicon capacitors
Appl. Phys. Lett. **93**, 213501 (2008); 10.1063/1.3021015

The improvement of retention time of metal-ferroelectric (Pb Zr 0.53 Ti 0.47 O 3) -insulator (Zr O 2) -semiconductor transistors and capacitors by leakage current reduction using surface treatment
Appl. Phys. Lett. **91**, 192906 (2007); 10.1063/1.2807842

The effect of band offset on the retention properties of metal-ferroelectric (Pb Zr 0.53 Ti 0.47 O 3) -insulator (Dy 2 O 3 , Y 2 O 3) -semiconductor capacitors and field effect transistors
Appl. Phys. Lett. **91**, 122902 (2007); 10.1063/1.2784203

Fabrication and characterization of metal-ferroelectric (Pb Zr 0.53 Ti 0.47 O 3) -insulator (Dy 2 O 3) -semiconductor capacitors for nonvolatile memory applications
Appl. Phys. Lett. **88**, 072917 (2006); 10.1063/1.2177549

Capacitance-voltage modeling of metal-ferroelectric-semiconductor capacitors based on epitaxial oxide heterostructures

Woong Choi,[1,2,a)] Sunkook Kim,[2] Yong Wan Jin,[2] Sang Yoon Lee,[2] and Timothy D. Sands[1,b)]

[1]*Department of Materials Science and Engineering, University of California, Berkeley, California 94720, USA*
[2]*Samsung Advanced Institute of Technology, Samsung Electronics, Yongin, Gyeonggi 446-712, Republic of Korea*

We report a quantitative investigation on the capacitance-voltage (*C-V*) modeling of metal-ferroelectric-semiconductor epitaxial heterostructures based on a theoretical model. Within the carrier concentration between 10^{17} and 10^{21} cm^{-3}, calculated *C-V* curves were consistent with measurements exhibiting from a significant asymmetry to a typical butterfly shape resembling that of a metal-ferroelectric-metal capacitor. The behavior of the *C-V* curves can be understood by the width of the depletion region and the extent of the depolarization field. These results suggest that quantitative understanding on the electrical behavior of oxide heterostructures is possible with *C-V* measurements with potentially important implications on their device applications. © *2011 American Institute of Physics.* [doi:10.1063/1.3561751]

Epitaxial oxide heterostructures are of great interest since the diverse properties of oxides and oxide superlattices can offer attractive possibilities for various device structures.[1,2] Special emphasis has been put on ferroelectric-semiconductor heterostructures, which permit nonvolatile memory elements with nondestructive readout, sensors, and tunable microwave devices. While the modulation of semiconductor conductivity by ferroelectric polarization has been investigated in several oxide systems such as $Pb(Zr,Ti)O_3$ (PZT)/(La,Ca)MnO$_3$ (LCMO),[3–5] or PZT/ZnO,[6–8] little attention has been given to their capacitance-voltage (*C-V*) characteristics. Unlike a silicon-based metal-ferroelectric-insulator-semiconductor (MFIS) structure, for which quantitative models have been developed to describe its *C-V* behavior,[9–12] no quantitative analysis on the *C-V* measurement has been reported so far for the metal-ferroelectric-semiconductor (MFS) epitaxial oxide heterostructures. In some cases, the measured *C-V* curve of the MFS structure exhibited the typical butterfly shape observed in a metal-ferroelectric-metal (MFM) capacitor.[3,4,13] However, in other cases, the shape of *C-V* curves was so asymmetrical that neither the MFM nor the MFIS model could adequately describe its behavior.[6–8] Furthermore, lack of quantitative understanding precluded the *C-V* measurement of the oxide heterostructure from providing valuable insight into the electrical properties, such as the carrier concentration in the semiconducting oxide, the width of a depletion layer, or the density of interface traps. In this study, we therefore attempt to deliver a quantitative modeling on the *C-V* characteristics of an MFS capacitor based on an epitaxial oxide heterostructure. We investigate *C-V* characteristics obtained by a simulation to demonstrate the feasibility of using the *C-V* measurement as a tool of understanding and predicting the

electrical behavior of the MFS epitaxial oxide heterostructure.

The MFS structure for the analysis is shown in Fig. 1(a) along with a simple equivalent circuit. The theory and the technique for the simulation are based on the model developed by Miller and McWhorter.[9] However, unlike their model, a semiconducting oxide (*p*-type) is used instead of silicon and no insulating layer exists between the ferroelectric and the semiconductor. If the flat band voltage is assumed to be zero and the interface trap density is negligible, the gate voltage V_g, divided between the semiconductor and the ferroelectric, is given by[9]

$$V_g = \phi_S - [Q_S + P(E_{FE})]d_{FE}/\varepsilon_0\varepsilon_{FE}, \tag{1}$$

where ϕ_S, Q_S, $P(E_{FE})$, ε_0, ε_{FE}, and d_{FE} are the surface potential, the surface charge in the semiconductor, the ferroelectric polarization as a function of the electric field, the permittivity of free space, the linear dielectric constant of the ferroelectric, and the thickness of the ferroelectric, respectively. The electric field in the ferroelectric layer is given by[9]

$$E_{FE} = -[Q_S + P(E_{FE})]/\varepsilon_0\varepsilon_{FE}. \tag{2}$$

If the semiconducting oxide is assumed to follow the conventional band description, the surface charge of the semiconductor Q_S is given as a function of the surface potential ϕ_S by[14]
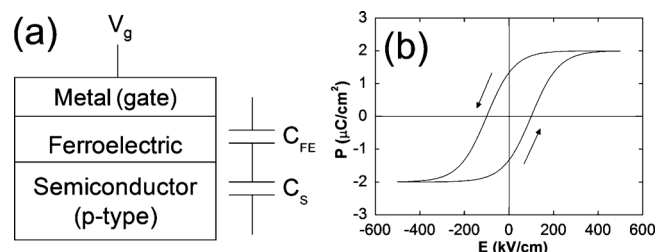

FIG. 1. (a) Schematic cross-section of the MFS capacitor along with an equivalent circuit. (b) The saturated hysteresis loop of ferroelectric polarization as a function of the electric field.

a)Electronic mail: woong1.choi@samsung.com.
b)Present address: School of Materials Engineering, School of Electrical and Computer Engineering, Purdue University, West Lafayette, Indiana 47907, USA.
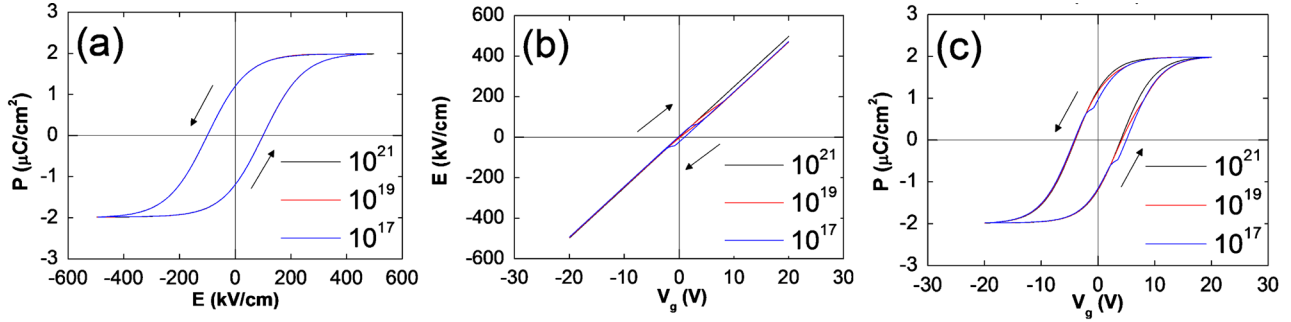
FIG. 2. (Color online) Simulation example of (a) P-E_{FE}, (b) E_{FE}-V_g, and (c) P-V_g in the MFS structure for different carrier concentrations (in cm^{-3}).

$$Q_S(\phi_S) = -Sgn(\phi_S)\frac{\sqrt{2}\varepsilon_0\varepsilon_s}{\beta L_B}\left[(e^{-\beta\phi_S}+\beta\phi_S-1)\right.$$
$$\left.+\left(\frac{n_i}{N_a}\right)^2(e^{\beta\phi_S}-\beta\phi_S-1)\right]^{1/2}, \tag{3}$$

where $Sgn(\phi_S)$ is the sign of ϕ_S, ε_S is the dielectric constant of the semiconductor, N_a is the carrier concentration, n_i is the intrinsic carrier concentration, $\beta \equiv q/kT$ (q: unit charge, k: Boltzmann's constant, and T: temperature), and the Debye length L_B is given by $(\varepsilon_0\varepsilon_S/\beta q N_a)^{1/2}$. The total capacitance per unit area of the MFS structure C_{total} is given by[14]

$$C_{total} = (C_S^{-1} + C_{FE}^{-1})^{-1}, \tag{4}$$

where the capacitance per unit area of the semiconductor C_S is given by[14] $C_S = -dQ_S/d\phi_S$ and the capacitance per unit area of the ferroelectric layer C_{FE} is given by[9] $C_{FE} = -d(Q_S + P)/dV_g = (\varepsilon_0\varepsilon_{FE} + dP/dE_{FE})/d_{FE}$. When the function $P(E_{FE})$ is known, Eqs. (1)–(4) completely describe the capacitor operation of the MFS structure in Fig. 1(a).[9,14] It needs to be mentioned that C_{FE} in the above equation is valid at a low frequency while the MFS C-V curves are typically measured at a high frequency. Hence, C_S will be constrained at its minimum value in depletion for the simulation.

The saturated polarization hysteresis loop shown in Fig. 1(b) can be expressed by[9] $P_{sat}^+(E_{FE}) = P_s \tanh[(E_{FE}-E_c)/2\delta]$ for the positive-going branch and $P_{sat}^-(E_{FE}) = P_s \tanh[(E_{FE}+E_c)/2\delta]$ for the negative-going branch, where $\delta = E_c/\ln[(1+P_r/P_s)/(1-P_r/P_s)]$ and P_S, P_r, and E_C correspond to the spontaneous polarization, the remanent polarization, and the coercive field, respectively. The derivative of the polarization is given by[9]

$$dP/dE_{FE} = \Gamma dP_{sat}/dE_{FE}, \tag{5}$$

where $\Gamma = 1 - \tanh\{[(P-P_{sat})/(\xi P_s - P)]^{1/2}\}$ and $\xi = 1$ when $dE_{FE}/dt > 0$ and $\xi = -1$ when $dE_{FE}/dt < 0$. $P(E_{FE})$ can then be obtained by integrating Eq. (5) with the sequence developed by Miller and McWhorter.[9] Once $P(E_{FE})$ is obtained, C_{total} can also be calculated as a function of V_g by Eq. (4). The parameters used to perform the analysis were $E_C = 100$ kV/cm, $P_S = 2$ μC/cm^2, $P_r = 1.33$ μC/cm^2, $d_{FE} = 400$ nm, $\varepsilon_{FE} = 130$, $N_a = 10^{17} - 10^{21}$ cm^{-3}, $n_i = 10^{10}$ cm^{-3}, $\varepsilon_S = 30$, and $T = 300$ K. The initial conditions are $V_g = 0$ and $P = 0$. The applied gate voltage was limited to ± 20 V.

The key of describing the capacitor operation, the polarization hysteresis loop as a function of the field in the ferroelectric layer $P(E_{FE})$, is shown in Fig. 2(a) for three different carrier concentrations (1×10^{17}, 1×10^{19}, and 1×10^{21} cm^{-3}). In contrast to silicon-based MFIS capacitors, which exhibit unsaturated hysteresis loops of the ferroelectric polarization,[9–11] the MFS capacitor based on the semiconducting oxide exhibits a saturated hysteresis loop. The MFS capacitors also exhibit a negligible depolarization field as the semiconducting oxide can fully compensate the ferroelectric polarization. This can be confirmed by the minimal hysteresis in the field in the ferroelectric with respect to gate bias in Fig. 2(b). The negligible existence of the depolarization field allows P_r in Fig. 2(c) to remain almost the same as that of the MFM capacitor. However, as the depolarization effect is pronounced for a semiconductor with lower concentration,[15] the existence of a minor depolarization field for $N_a = 10^{17}$ cm^{-3} causes slightly reduced P_r.

In MFIS capacitors, the insulating layer between the ferroelectric and the semiconductor imposes the following electrostatic boundary condition that must be satisfied at the dielectric layer interface,[9] $\varepsilon_0\varepsilon_{FE}E_{FE} + P = \varepsilon_0\varepsilon_I E_I$, where ε_I and E_I are the dielectric constant and the field in the insulator;
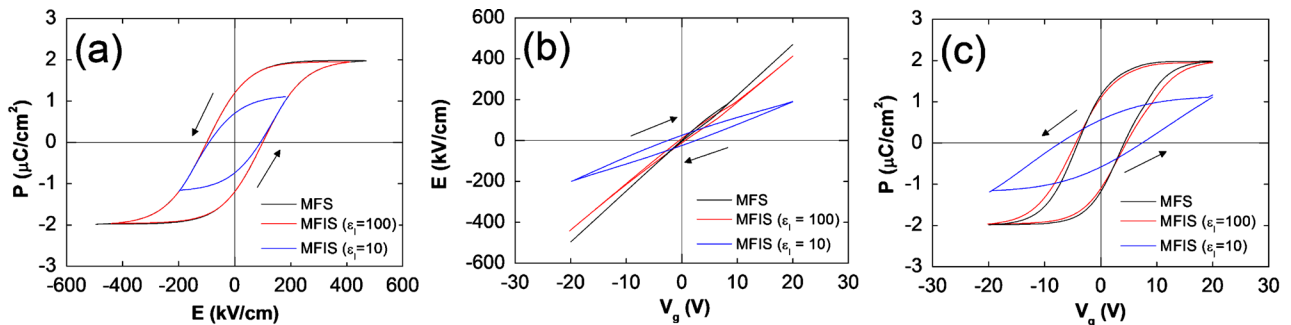

FIG. 3. (Color online) Simulation example of (a) P-E_{FE}, (b) E_{FE}-V_g, and (c) P-V_g in the MFIS structure for $\varepsilon_I = 100$ and $\varepsilon_I = 10$. Results in the MFS structure are also shown for comparison.
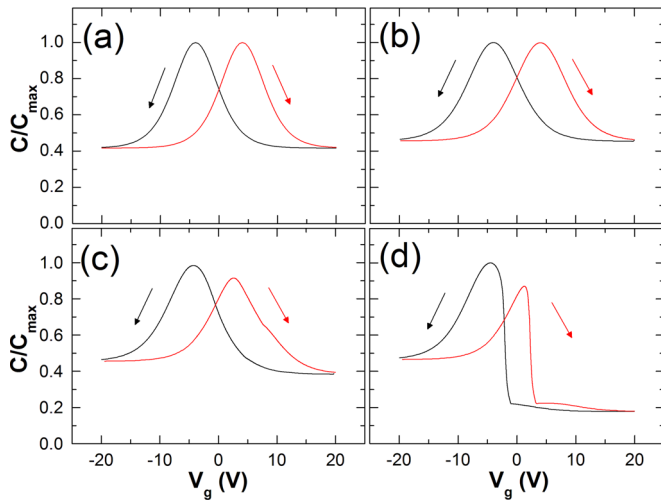
FIG. 4. (Color online) C-V curves of (a) the MFM capacitors and the MFS capacitors with the carrier concentration of (b) 10^{21}, (c) 10^{19}, and (d) 10^{17} cm^{-3} in the semiconductor. As the carrier concentration increases in the MFS structure, the contribution of C_S decreases in depletion making the shape of the C-V curves similar to that of the MFM capacitor.

respectively. Because a typical insulator layer does not provide enough charges to compensate the polarization in the ferroelectric layer, the depolarization field is formed to reduce the ferroelectric polarization (hence, resulting in an unsaturated polarization hysteresis loop). The effect of the insulator layer in the MFIS structure can be seen in Fig. 3, where we calculated the ferroelectric polarization and the depolarization field of the MFIS structure for $\varepsilon_I = 10$ and 100, respectively. (In both cases, the insulator is 30 nm thick and $N_a = 1 \times 10^{19}$ cm^{-3}.) When the insulator layer can compensate the polarization ($\varepsilon_I = 100$), the depolarization field becomes negligible resulting in the saturated polarization. However, the ferroelectric polarization becomes unsaturated when the insulator layer cannot compensate the polarization ($\varepsilon_I = 10$). The clockwise hysteresis loop in Fig. 3(b) clearly shows the formation of the depolarization field.

Figure 4 shows the C-V curves of the MFS capacitor for three different carrier concentrations (1×10^{17}, 1×10^{19}, and 1×10^{21} cm^{-3}), along with those of the MFM capacitor. As the maximum width of a depletion layer (W_{max}) in a semiconductor is given by $(2\varepsilon_0\varepsilon_S\phi_S/qN_a)^{1/2}$ and $C_S = \varepsilon_0\varepsilon_S/W_{max}$,[14] Eq. (4) implies a strong influence of N_a on C_{total}. As the semiconducting oxide behaves like a metal for $N_a = 1 \times 10^{21}$ cm^{-3} ($W_{max} < 1$ nm), C_{total} of the MFS capacitor in Fig. 4(b) resembles that of the MFM capacitor in Fig. 4(a). Similar C-V curves were reported in a PZT/LCMO system.[4] When $N_a = 1 \times 10^{19}$ cm^{-3} ($W_{max} \sim 18$ nm), C_{total} in Fig. 4(c) becomes asymmetrical with respect to the polarity of the applied voltage; the capacitance decreased by $\sim$17% under positive bias due to the formation of the depletion layer. In a p-type semiconductor such as LCMO or LaVO$_3$, the depletion layer in the semiconductor forms at positive bias.[3,16] (In an n-type semiconductor such as ZnO, the depletion layer forms at negative bias.) The formation of the depletion layer contributes an additional capacitance in series with that of the ferroelectric, reducing C_{total} at positive voltages. Similar C-V curves were reported in PZT/LCMO[3] and (Pb,La)(Zr,Ti)O$_3$/LaVO$_3$ systems.[13] When $N_a = 1$

$\times 10^{17}$ cm^{-3} ($W_{max} \sim 156$ nm), C_{total} decreases by $\sim$62% under positive voltages in Fig. 4(d), indicating a strong dependence of C_{total} on N_a. Such a significant decrease in capacitance was observed in PZT/ZnO systems.[7,8]

It needs to be mentioned that, for silicon-based MFIS capacitors, C_{total} represents C_{FE} in accumulation and C_S in depletion and inversion. C_{FE} is independent of the voltage in MFIS structures because the polarization hysteresis loop becomes unsaturated for typical ferroelectric materials. The effect of C_S to C_{total} is conspicuous in depletion and weak inversion, as the thick depletion layer, which is on the order of 1 μm for typical doping levels (10^{14}–10^{16} cm^{-3}),[14] makes the contribution of C_S predominant. However, in semiconducting oxide-based MFS structures, C_{FE} in accumulation maintains its field-dependent characteristics due to the saturated ferroelectric polarization. Furthermore, the high carrier concentration in typical semiconducting oxides (10^{19}–10^{22} cm^{-3}) induces a very thin depletion layer,[17] which results in the less conspicuous contribution of C_S to C_{total} in Fig. 4(c) than that in a silicon-based MFIS capacitor. The dominant contribution of C_S to C_{total} cannot be observed until the thickness of the depletion layer becomes comparable with that of silicon in Fig. 4(d).

In summary, we investigated the C-V modeling of MFS capacitors based on epitaxial oxide heterostructures. Unlike MFIS capacitors, MFS capacitors showed saturated hysteresis loops of the ferroelectric polarization as a function of the applied field. The C-V curves based on the Miller–McWhorter model showed good agreements with the measurement reported in literature. Between the carrier concentration of 10^{17} and 10^{21} cm^{-3}, the shape of the C-V curves exhibited a significant asymmetry at low carrier concentrations and it resembled that of the MFM capacitor at high carrier concentrations. These results demonstrate the feasibility of using the C-V measurement as a tool of analyzing the electrical behavior of oxide heterostructures, providing potentially important implications on their device applications.

[1]R. Ramesh and D. G. Schlom, MRS Bull. **33**, 1006 (2008).
[2]J. Mannhart, D. H. A. Blank, H. Y. Hwang, A. J. Milis, and J.-M. Triscone, MRS Bull. **33**, 1027 (2008).
[3]S. Mathews, R. Ramesh, T. Venkatesan, and J. Benedetto, Science **276**, 238 (1997).
[4]A. M. Grishin, S. I. Khartsev, and P. Johnsson, Appl. Phys. Lett. **74**, 1015 (1999).
[5]T. Zhao, S. B. Ogale, S. R. Shinde, R. Ramesh, R. Droopad, J. Yu, K. Eisenbeiser, and J. Misewich, Appl. Phys. Lett. **84**, 750 (2004).
[6]E. Cagin, D. Y. Chen, J. J. Siddiqui, and J. D. Phillips, J. Phys. D: Appl. Phys. **40**, 2430 (2007).
[7]Y. Kato, Y. Kaneko, H. Tanaka, and Y. Shimada, Jpn. J. Appl. Phys. **47**, 2719 (2008).
[8]L. Pintilie, C. Dragoi, R. Radu, A. Costinoaia, V. Stancu, and I. Pintilie, Appl. Phys. Lett. **96**, 012903 (2010).
[9]S. L. Miller and P. J. McWhorter, J. Appl. Phys. **72**, 5999 (1992).
[10]M. Liu, H. K. Kim, and J. Blachere, J. Appl. Phys. **91**, 5985 (2002).
[11]H.-T. Lue, C.-J. Wu, and T.-Y. Tseng, IEEE Trans. Electron Devices **49**, 1790 (2002).
[12]T. J. Reece and S. Ducharme, J. Appl. Phys. **106**, 124505 (2009).
[13]W. Choi and T. Sands, J. Appl. Phys. **93**, 4761 (2003).
[14]E. Nicollian and J. Brew, *MOS (Metal Oxide Semiconductor) Physics and Technology* (Wiley, New York, 1982).
[15]L. S. Berman, Semiconductors **35**, 193 (2001).
[16]W. Choi, S. Y. Lee, and T. D. Sands, Appl. Phys. Lett. **96**, 212903 (2010).
[17]C. H. Ahn, J.-M. Triscone, and J. Mannhart, Nature (London) **424**, 1015 (2003).